Journal of Ovarian Research

RESEARCH

Open Access

Network pharmacology and experimental validation to elucidate the mechanism of the treatment of polycystic ovary syndrome with insulin resistance by Resina Draconis

Jing Wang[1,2,3†], Yehao Luo[4†], Yueting Liu[1,2], Xiusong Tang[1,2], Jianhui Gu[1,2], Zheng Huang[1,2], Ting Lv[1,2], Jun Luo[5*] and Gang Fang[1,2*]

Abstract

Background Resina Draconis(RD) is a traditional Chinese medicine that activates blood circulation and removes blood stasis. Modern pharmacological studies have proved that RD has hypoglycaemic, pancreatic islets-protective, oestrogenic activity, anti-inflammatory, antibacterial and anti-tumour effects. Studies have shown that insulin resistance (IR) is the core pathological mechanism of polycystic ovary syndrome (PCOS), and RD can lower blood glucose to ameliorate IR, which has achieved significant results in the treatment of diabetes. However, the mechanism of action of RD in the treatment of PCOS-IR is still unclear.

Methods Network pharmacology analysis was used to predict the potential therapeutic targets of the active ingredients of RD. Experimental validation used a rat model of insulin resistance in PCOS; PCOS-IR symptoms were assessed, ovarian pathology was evaluated, and serum levels of insulin and sex hormones were determined. Expression levels of the PI3K, p-PI3K, Akt, p-Akt, GLUT4, FOXO3a, and P27 proteins were also measured in rat ovaries, along with mRNA expression levels of PI3K, Akt, GLUT4, FOXO3a, and P27.

Results Network pharmacological analyses indicated that the PI3K/Akt signalling pathway may play an important role in the treatment of PCOS-IR rats with RD. Experiments in PCOS-IR rats showed that RD significantly reversed insulin resistance, improved pathological changes in the ovaries, increased serum levels of follicle stimulating hormone (FSH) and estradiol (E2), and decreased levels of luteinizing hormone (LH), testosterone (T) and insulin. In addition, RD increased the levels of PI3K, p-PI3K, Akt, p-Akt and GLUT4, and decreased the levels of FOXO3a and P27 in the ovarian tissues of PCOS-IR rats, suggesting that RD may improve the symptoms of PCOS-IR in rats through the PI3K/Akt signalling pathway.

[†]Jing Wang and Yehao Luo contributed equally to this work.

*Correspondence:
Jun Luo
jluo@gxtcmu.edu.cn
Gang Fang
fglzyznn@gxtcmu.edu.cn

Full list of author information is available at the end of the article

Conclusion RD might improve insulin resistance and ovarian function in PCOS-IR by upregulating PI3K, p-PI3K, Akt, p-Akt and GLUT4 expression and downregulating FOXO3a and P27, thereby activating the PI3K/Akt signaling pathway. RD also regulated the LH/FSH ratio, increased E2 levels, reduced LH and T levels, and alleviated PCOS-IR symptoms in a rat PCOS-IR model.

Keywords Network pharmacology, Resina Draconis, Polycystic ovary syndrome, Insulin resistance, PI3K/Akt signaling pathway

Introduction

Polycystic ovary syndrome (PCOS), a common endocrine disorder affecting women of reproductive age [1], is characterized by reproductive disturbances and metabolic abnormalities [2]. Clinical manifestations often include enlarged ovaries with multiple cysts, menstrual cycle disturbances, ovulatory dysfunction, hyperandrogenism, and IR [3]. IR exacerbates PCOS [4], as insulin affects steroidogenesis in the ovaries [5], directly regulates ovarian cell differentiation, and increases serum androgen levels [6, 7]. Currently, metformin is the first-line drug for the treatment of insulin resistance in polycystic ovary syndrome (PCOS-IR) [8], but in clinical practice, gastrointestinal symptoms such as nausea, abdominal pain, abdominal distension, diarrhea and other gastrointestinal symptoms, and in severe cases, renal function and lactic acidosis may be impaired [9]. Diane-35, which is a drug that can improve estrogen-progesterone cycle and thereby restore ovulation and menstrual cycle, is usually used in combination with metformin to improve glucose metabolism and lipid metabolism and promote ovulation [10]. Therefore, we aimed to find effective natural agents for the treatment of PCOS-IR.

Resina Draconis (RD), a traditional Chinese medicine (TCM), is renowned for being the "sacred herb for promoting blood circulation" [11]. It is derived primarily from resins extracted from the palm species Daemonorops and the Dracaena (dragon tree) plant, a member of the lily family [12]. Modern pharmacological research confirms the various beneficial functions of RD, which include the ability to reduce blood glucose levels in rats, protect pancreatic islets, exhibit estrogenic activity, improve lipid metabolism, and enhance the microcirculation [13–15].

An interdisciplinary field based on systems biology, network informatics, and the specific selection of signaling nodes for multi-target drug molecule design [16], network pharmacology is a promising method for exploring the mechanisms of drug therapy [17]. Network pharmacology research has multiple aims: to predict the target profile and pharmacological effects of TCM compounds and formulations; to elucidate synergistic drug–gene–disease associations; to screen synergistic compound composition in TCM prescriptions in a high-throughput manner; and to explain the combination patterns and network regulation effects of TCM formulations [18]. Significant success has been achieved in screening effective ingredients and therapeutic targets at the system level, thereby improving drug efficacy and reducing side effects [19]. Therefore, network pharmacology approaches can serve as an effective method for exploring the potential mechanisms of action of RD in treating PCOS-IR.

This study explored the effect of RD on PCOS-IR, and the potential mechanism by which RD improves PCOS-IR symptoms, using network pharmacology combined with an experimental PCOS-IR model in rats.

Materials and methods

The mechanism of action of RD in improving PCOS-IR symptoms: network Pharmacology

Screening active compounds in RD and predicting targets

We searched the literature related to RD in the ScienceDirect (https://www.sciencedirect.com/), PubMed (https://pubmed.ncbi.nlm.nih.gov/), and Web of Science (https://webofscience.clarivate.cn/) databases to identify the effective active ingredients of RD. The chemical structures of these compounds were identified using PubChem (https://pubchem.ncbi.nlm.nih.gov/). Subsequently, potential active compounds were predicted using SwissADME (http://www.swissadme.ch/). Compounds with high gastrointestinal (GI) absorption and more than three"Yes, 0 violation"in Druglikeness (DL) analysis were screened out as bioactive compounds for subsequent analysis. The Swiss Target Prediction database (http://www.swisstargetprediction.ch/) was then used to predict the potential targets of these active compounds; targets with confidence values of <0 were removed to obtain relevant potential target genes.

Screening target genes of PCOS-IR

Target genes associated with PCOS-IR were screened from the GeneCards (https://www.genecards.org/), PharmGkb (https://www.pharmgkb.org/), DrugBank (https://go.drugbank.com/), OMIM (https://omim.org/), and DisGeNET (https://www.disgenet.org/) databases using the keywords "Polycystic Ovary Syndrome," "Insulin Resistance," "PCOS" and "IR." Potential PCOS-IR targets were merged, and duplicate genes were removed.

Constructing a protein-protein interaction (PPI) network

A Venn diagram analysis was conducted to identify intersecting RD target genes and PCOS-IR target genes. The intersecting target genes were then imported into the STRING database (https://cn.string-db.org/), using a minimum required interaction score of > 0.9, to obtain protein-protein interaction (PPI) information. Subsequently, a PPI network was constructed using Cytoscape 3.7.2.

GO and KEGG enrichment analysis

The Gene Ontology (GO) database (https://geneontology.org/) is used for analyzing the cellular components (CC), molecular functions (MF), and biological processes (BP) in genetic information. GO analysis therefore provides a broad understanding of the biological functions, pathways, and locations that are enriched in cells. The Kyoto Encyclopedia of Genes and Genomes (KEGG) (https://www.genome.jp/kegg/) is a database for systematic gene analysis. GO and KEGG enrichment analyses were conducted for the intersecting RD and PCOS-IR target genes using the "clusterProfiler," "org.Hs.eg.db," and "ggplot2" packages in the R programming language; significance thresholds of $p < 0.05$ and $q < 0.01$ were used to identify the GO domains (CC, MF, and BP) and KEGG signaling pathways associated with each intersecting target gene.

Constructing the compound–target–pathway network

Using CytoScape 3.7.2 to construct the compound-target-pathway network, the top 20 KEGG signaling pathways and their corresponding targets were imported into CytoScape 3.7.2, and a main compound-target-pathway network diagram for RD treatment of PCOS-IR was drawn.

Reagents

Rabbit anti-PI3K (AF6241), rabbit anti-p-PI3K (AF3241), rabbit anti-AKT (AF6261), rabbit anti-p-AKT (AF0016), β-actin (AF7018), P27KIP1 (AF6324), and GLUT4 (AF5386) were all purchased from Affinity Biosciences (Jiangsu, China). FOXO3a (K001577P) was purchased from Solarbio (Beijing, China). Horseradish peroxidase (HRP) (K1224) conjugated secondary antibody was purchased from APExBIO (Houston, Texas, USA). Efficient RIPA (RIPA: PMSF = 100:1,v/v) tissue lysis buffer kit and a BCA protein assay kit were purchased from Solarbio (BeiJing, China). Rat follicle-stimulating hormone (FSH) (CEA830Ra), luteinizing hormone (LH) (CEA441Ra), testosterone (T) (CEA458Ge), estrogen (E2) (CEA461Ge) and insulin (INS) (CEA448Ra) enzyme-linked immunosorbent assay (ELISA) kits were purchased from Wuhan Yunkelong Technology Co., Ltd. (Wuhan, China). RD was purchased from Guangxi University of Chinese Medicine Bai Nian Le Pharmaceutical Co., Ltd (NanNing, China). Letrozole was purchased from Zhejiang Haizheng Pharmaceutical Co., Ltd (ZheJiang, China), while Diane-35 (cyproterone acetate and ethinyl estradiol) and metformin were purchased from Bayer Healthcare Co., Ltd (GuangZhou, China) and Hebei Tiancheng Pharmaceutical Co., Ltd (HeBei, China), respectively. The HyperScript III RT SuperMix for qPCR with gDNA Remover kit (R201-02, EnzyArtisan, China) and the 2×S6 Universal SYBR qPCR Mix kit (Q204-01, EnzyArtisan, China) were both purchased from EnzyArtisan (ShangHai, China).

Experimental validation

Animals

A total of 90 female Sprague-Dawley (SD) rats, each aged 3 weeks and weighing 70–90 g were purchased from Hunan SJA Laboratory Animal Co., Ltd (HuNan, China). All animals were housed and handled in accordance with guidelines approved by the Ethics Committee of Guangxi University of Chinese Medicine (Approval No.: DW20240603-142). The rats were kept in a room maintained at 22 °C with a 12-hour light/dark cycle, and they had free access to food and water for a one-week acclimatization period prior to experimentation.

Animal modeling and experimental grouping

Rats were randomly divided into two groups: the normal group (normal; $n = 10$) and the Modeling group ($n = 80$). Rats in the Modeling group were given letrozole solution (letrozole dissolved in 0.5% carboxymethyl cellulose sodium solution) once daily at 10 a.m. for 21 days, in combination with a high-fat diet, to induce the PCOS-IR model. Letrozole solution was administered via gastric gavage at a dose of 1 mg/kg/d [20]. Normal rats were given an equal volume of 0.5% carboxymethyl cellulose sodium solution via gastric gavage once daily at 10 a.m. and fed a normal diet for 21 days.

Fasting began at 8 p.m. on the evening of the 21st day of modeling, and fasting blood glucose (FBG) was measured from samples drawn from the tail vein at 8 a.m. the following morning. Blood samples were also collected to determine serum fasting insulin levels. IR was calculated using the Homeostatic Model Assessment of IR (HOMA-IR), where the HOMA-IR score = FBG×INS/22.5. Fifty rats with a HOMA-IR score of > 2.8 were selected to be the PCOS-IR model for subsequent experiments [21]. The 50 PCOS-IR rats were randomly and equally divided into five groups: the Model group; the Metformin group (ME; 156 mg/kg/d); the RD group (312 mg/kg/d); the Metformin + Diane-35 group (MED-35; Diane-35: 0.2 mg/kg/d + ME: 156 mg/kg/d); and the RD + Diane-35 group (RDD-35; Diane-35: 0.2 mg/kg/d + RD: 312 mg/kg/d), with 10 rats in each group. Each treatment group was given the corresponding drugs once daily at 10 a.m. via gastric gavage each day, 21 consecutive day, and in

the combination group, the MED-35 and RDD-35 groups were given one drug by gavage and followed by another drug by gavage. The Normal and Model groups were given an equal volume of normal saline via gastric gavage. After the last treatment administration, rats fasted for 12 h and their body weights and FBG were measured.

Blood and ovary tissues sampling

Rats were anesthetized with 3% sodium pentobarbital solution (0.2 mL/100 g) via intraperitoneal injection. Blood was collected from the abdominal aorta, and ovary tissue was collected. Blood samples were allowed to stand at room temperature for 2 h before being centrifuged at 3000 rpm for 20 min, following which serum samples were collected and stored at − 80 °C for subsequent experimental analysis. Following abdominal blood collection, the ovaries were rapidly removed and weighed, and the average weight of both ovaries was calculated for each rat and used as the ovarian weight for subsequent calculations. The ovarian organ index was calculated as follows for each rat: ovarian index = ovarian weight/rat weight × 10^{-3} [22]. The longest (L) and shortest (S) diameters of the ovaries were measured with a vernier caliper, and the ovarian area (area = L × S) and ovarian volume (volume = 4.19 × $[(L+S)/2]^3$) were calculated [23]. Left ovarian tissue was fixed in 4% paraformaldehyde for 24 h and then embedded in paraffin, while right ovarian tissue was stored in liquid nitrogen for subsequent experiments. All procedures were performed on ice.

Body weight changes and estrous cycle monitoring

The rats' body weights were measured before modeling and then once weekly (every Sunday at 10 a.m.) during modeling and treatment. Starting on the 10th day of modeling, vaginal smears were taken daily at 10 a.m. to observe changes in vaginal exfoliated cells and thus monitor the estrous cycle in each group of rats.Rats fasted for 12 h before each weight measurement.

Enzyme-linked immunosorbent assay

A rat insulin ELISA kit was used to detect fasting insulin levels in the collected rat serum samples. Insulin resistance was determined using the HOMA-IR index. ELISA kits were also used to detect FSH, LH, T, and E2 levels in rat serum. All ELISA operations were carried out according to the manufacturer's instructions.

Histopathological analysis

The ovarian tissues embedded in paraffin were cut into thin (4 μm) sections, dewaxed with xylene and ethanol, and stained with hematoxylin-eosin (H&E). The histological characteristics of each sample were observed and analyzed under an Olympus BX51 microscope (Olympus, Tokyo, Japan).

Western blot

The ovarian tissues were thawed and mixed with high-efficiency RIPA tissue lysis buffer at a ratio of 1 mg:100 μl. Protein was extracted from the ovarian samples and the protein concentration determined using a BCA protein assay kit. Proteins were separated by electrophoresis and transferred to PVDF membranes. Rabbit anti-PI3K, rabbit anti-p-PI3K, rabbit anti-AKT, rabbit anti-p-AKT, rabbit anti-GLUT4, rabbit anti-FOXO3a, and rabbit anti-P27 antibodies were diluted 1:1000 in 5% skim milk, and the PVDF membranes were incubated overnight on ice in a shaker with the corresponding primary antibodies. The membranes were then incubated with HRP-conjugated secondary antibodies at a dilution of 1:10,000 at room temperature for 2 h. Protein bands were visualized using Proteinsimple (FluorChem E, San Jose, CA, USA), and the grayscale values of each protein were calculated using ImageJ.

Total RNA extraction and real-time quantitative reverse transcription polymerase chain reaction (RT-qPCR)

Total RNA was extracted from ovarian tissue using chloroform and TriQuick reagent. Subsequently, cDNA was synthesized by reverse transcription using the HyperScript III RT SuperMix for qPCR kit, and qPCR analysis was performed with the real-time LightCycler PCR system (Roche Diagnostics, Indiana, USA) using a 2×S6 Universal SYBR qPCR Mix kit. The thermal cycling conditions were as follows: 95 °C for 30 s, followed by denaturation at 95 °C for 10 s, followed by annealing at 60 °C for 30 s, for 40 cycles. The relative expression levels of genes in each sample were normalized to β-actin levels using the $2^{-\triangle\triangle Ct}$ method (Table 1).

Table 1 Primer sequence

Gene name	Forward primer	Reverse primer
PI3K	GTGAGGAACGAAGAATGG	CAAAAACAGTGAGGTCGG
AKt	GTCCCCACTCAACAACTTCT	CCACTCTTCCCGCTCCT
GLUT4	CAGGCCGGGACACTATACCCTAT	GCCAAGCACAGCTGAGAATACAG
FOXO3a	CATTCCAACTTACGGAGCGGCAC	GAAGCAAACGGACAAGAGAGTGG
P27	TGGAAAGCGGTCTGCAAGTG	TCACTGTCACATTCAGGGGC
β-actin	ACATCCGTAAAGACCTCTATGCC	TACTCCTGCTTGCTGATCCAC

Statistical analysis

Data were analyzed using SPSS software (version 27.0). All results are expressed as mean ± standard deviations(SD). Student's t-tests were used for comparisons between two groups, while one-way analysis of variance (ANOVA) with Dunnett's test was used to compare multiple groups. P values of < 0.05 were considered statistically significant.

Results

Predicting potential targets of RD in PCOS-IR: network pharmacology

Active compounds and targets of RD

After consulting the relevant literature, we identified 221 effective active ingredients of RD (Supplementary file 1). The chemical structures of these compounds were determined using PubChem. After screening the compounds using SwissADME criteria for high GI absorption, a total of 121 bioactive compounds were identified.Subsequently, using the Swiss Target Prediction database, we identified 710 potential targets related to these bioactive compounds (Supplementary file 2).

Candidate targets and PPI network analysis

Disease target genes collected from five databases (GeneCards, PharmGkb, DrugBank, OMIM, and DisGeNET) were merged and, following removal of duplicates, 4166 disease target genes were identified (Supplementary file 3). A Venn diagram was then created to identify the intersection of target genes for the effective ingredients of RD and target genes for PCOS-IR. A total of 407 intersecting target genes were identified (Fig. 1; Supplementary file 4).

The 407 intersecting target genes were then imported into the STRING database, and PPI information was obtained based on a minimum required interaction value of > 0.9. A PPI network graph consisting of 327 nodes and 1204 edges was generated using CytoScape (Fig. 2).

Fig. 1 Venn diagram illustrating potential target genes for the treatment of PCOS-IR by RD

GO and KEGG enrichment analysis

GO enrichment analysis identified 3,172 BP, 130 CC, and 285 MF (Supplementary file 5). The top 10 GO terms were visually depicted in bar charts, as shown in Fig. 3. The BP terms were primarily related to the cellular response to peptide, response to peptide hormone, cellular response to peptide hormone stimulus, peptidyl-serine phosphorylation, and response to xenobiotic stimulus. The CC terms were focused on membrane raft, membrane microdomain, neuronal cell body, protein kinase complex, and glutamatergic synapse. The MF terms were mainly associated with postsynaptic cytosol, protein serine/threonine kinase activity, protein tyrosine kinase activity, protein serine kinase activity, and transmembrane receptor protein kinase activity.

KEGG pathway enrichment analysis identified 195 KEGG signaling pathways related to the core targets (Supplementary file 6), and the 20 most significant pathways were visualized in a bubble chart (Fig. 4). The top 5 signaling pathways most related to treating PCOS-IR with RD were the PI3K-Akt signaling pathway, chemical carcinogenesis–receptor activation, neuroactive ligand-receptor interaction, proteoglycans in cancer, and the main calcium signaling pathway.

A compound–target–pathway network was constructed, incorporating the top 20 KEGG signaling pathways and 91 genes corresponding to the 121 bioactive compounds identified in RD. This compound–target–pathway network comprised 232 nodes and 2707 edges (Fig. 5; Supplementary file 7), and network analysis suggested that treating PCOS-IR with RD involves multiple components, targets, and pathways. With 50 genes, the PI3K/Akt signaling pathway ranks as the most significant among all pathways related to PCOS-IR. This signaling pathway is involved in processes such as cell survival, proliferation, growth, and metabolism, which explains its relevance in PCOS-IR and its treatment.

Experimental validation of RD treatment in PCOS-IR

Vaginal smears

Vaginal cytology smears indicated that normal rats have a regular estrous cycle, which includes proestrus, estrus, metestrus, and diestrus phases, with an estrous cycle length of 4–5 days (Fig. 6). In contrast, vaginal smears of PCOS-IR rats showed a large number of leukocytes with fewer nucleated epithelial cells and keratinized cells, indicating that PCOS-IR rats were persistently in diestrus without ovulation. A normal estrous cycle was observed in all treatment groups (ME, RD, MED-35, RDD-35) after treatment (Fig. 7A and G).

RD decreases the body weight of PCOS-IR rats

Compared with the normal group, rats in the model group showed a significant increase in body weight from

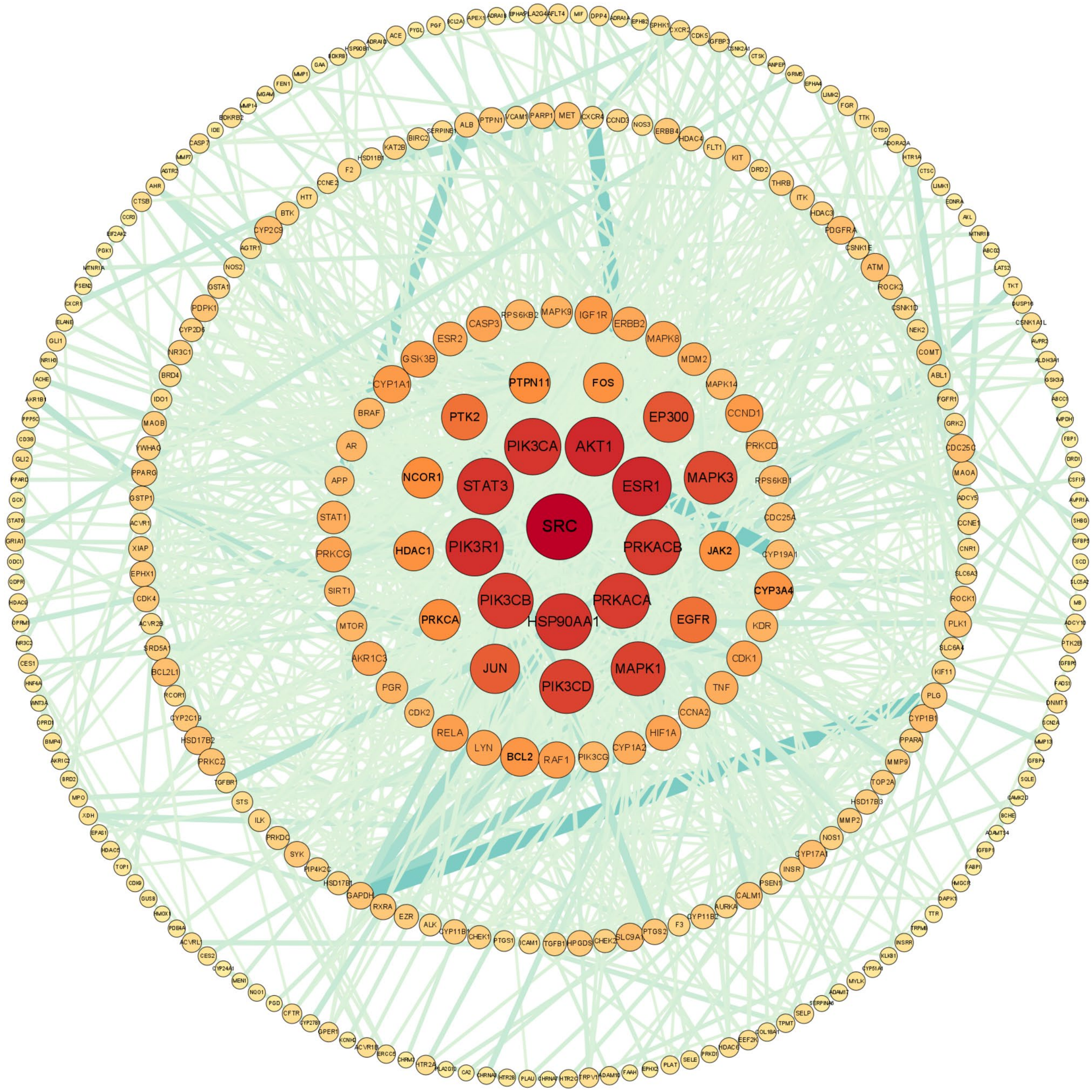

Fig. 2 PPI network of key drug and disease targets. Circular nodes represent targets. The larger and darker the node, the higher the degree value. Thicker edges indicate higher combined scores

week 1 to week 3 (Fig. 8A and C). Compared with the model group (untreated modeled rats), rats in all treatment groups showed a decrease in body weight in the first week of treatment(Fig. 8A), but without statistical significance. In the second week of treatment, rats in the MED-35 group showed a significant decrease in body weight, and the RDD-35 group also showed a significant decrease, while the ME group and RD group experienced weight loss but without statistical significance(Fig. 8B). In the third week of treatment, compared with the model group, all treatment groups (ME, RD, MED-35, RDD-35) had significant weight reduction (Fig. 8C). These results indicate that treatment with metformin or RD, either alone or in combination with Diane-35, can reduce body weight in these animals, with combined use producing significantly greater effects than monotherapy. Additionally, the effect of RD on the body weight of PCOS-IR rats was comparable to that of metformin, and the effect of RD combined with Diane-35 was comparable to that of metformin combined with Diane-35(Fig. 8A and C).

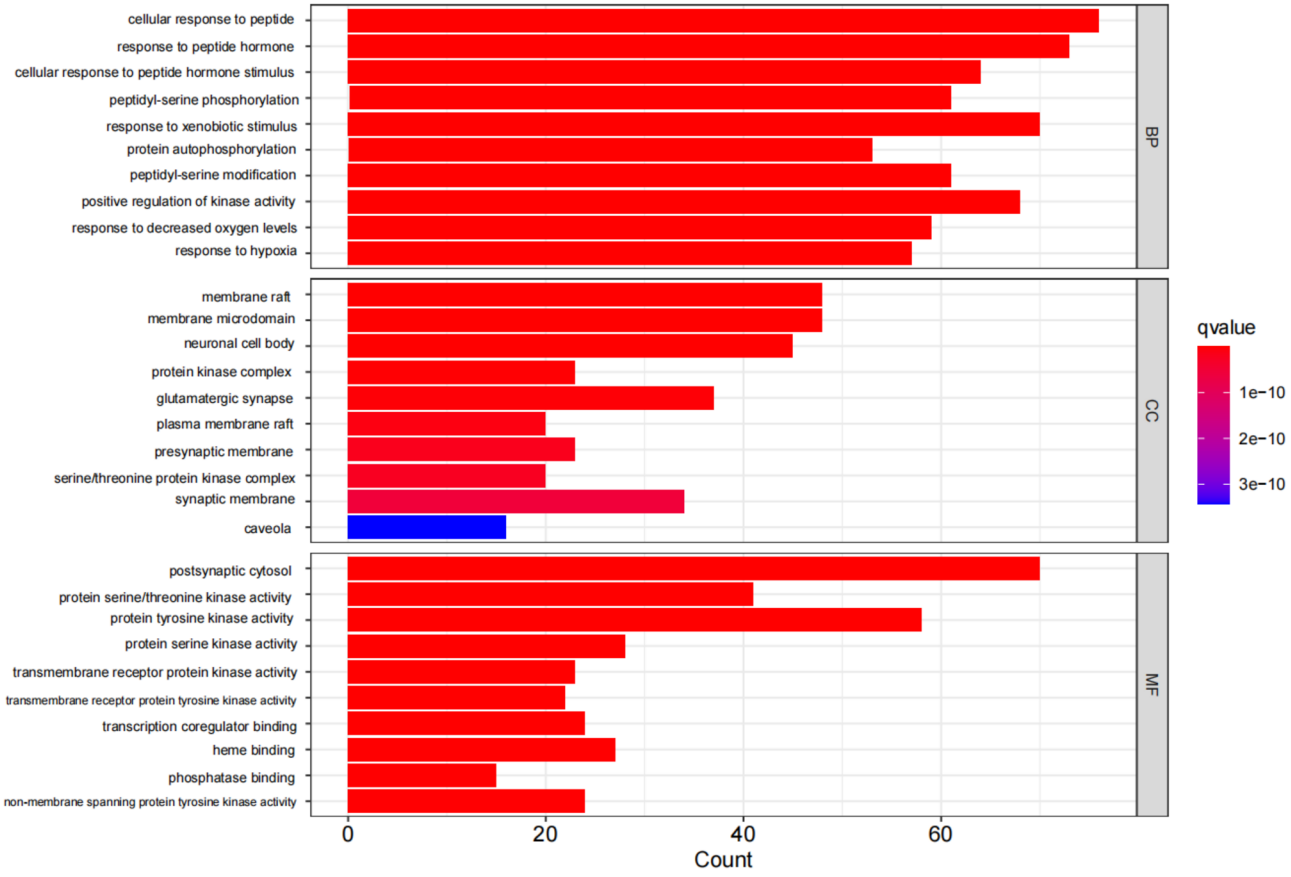

Fig. 3 GO enrichment analysis results (the top 10 core targets of RD in treating PCOS-IR). The longer the bar, the greater the number of enrichments; the redder the color, the more significant the enrichment

RD decreases the ovarian index, area, and volume in PCOS-IR rats

Compared with normal rats, ovarian index, area, and volume were significantly increased (Fig. 9A and C) in model group rats. Compared with the model group, rats treated with ME or RD showed a significant decrease in ovarian index, area, and volume (Fig. 9A and C). The MED-35 and RDD-35 groups also exhibited a significant reduction in ovarian index, area, and volume compared with the model group (Fig. 9A and C). There were no significant differences in these measures between the ME and RD groups or between the MED-35 and RDD-35 groups; however, ovarian area and volume were significantly smaller in the MED-35 group compared with the ME group (Fig. 9B and C) and in the RDD-35 group compared with the RD group (Fig. 9B and C). These results suggest that letrozole combined with a high-fat diet increases the ovarian index and enlarges ovarian volume and area in PCOS-IR rats. The findings also indicate that RD can improve these pathological changes, and that a combination of RD and Diane-35 is superior to RD alone. Additionally, the differences in these pathological changes between RD and ME were not statistically significant (Fig. 9A and C), suggesting that the efficacy of RD or ME combined with Diane-35 is more effective than either RD or ME alone (Fig. 9A and C).

RD decreases the pathological ovarian changes in PCOS-IR rats

The ovaries of rats in the normal group (Fig. 10A) showed follicles at different stages of development, with granulosa cells presenting a multi-layered structure, intact morphology, uniform distribution, and higher corpus luteum number. In contrast, ovaries from rats in the Model group (Fig. 10B) exhibited cystic expansion of ovarian follicles, loss of oocytes, and granulosa cells with fewer layers irregular distribution, and massive decrease in corpus luteum. Compared with the Model group, ovaries from the ME (Fig. 10C) and RD (Fig. 10D) groups had smaller ovarian follicles and showed the presence of oocytes as well as a higher number of granulosa cell layers, and increased number of corpus luteums. In the MED-35 (Fig. 10E) and RDD-35 (Fig. 10F) groups, follicles at different stages were observed, with granulosa cells showing an increased number of layers, regular morphology, and uniform distribution, and increased

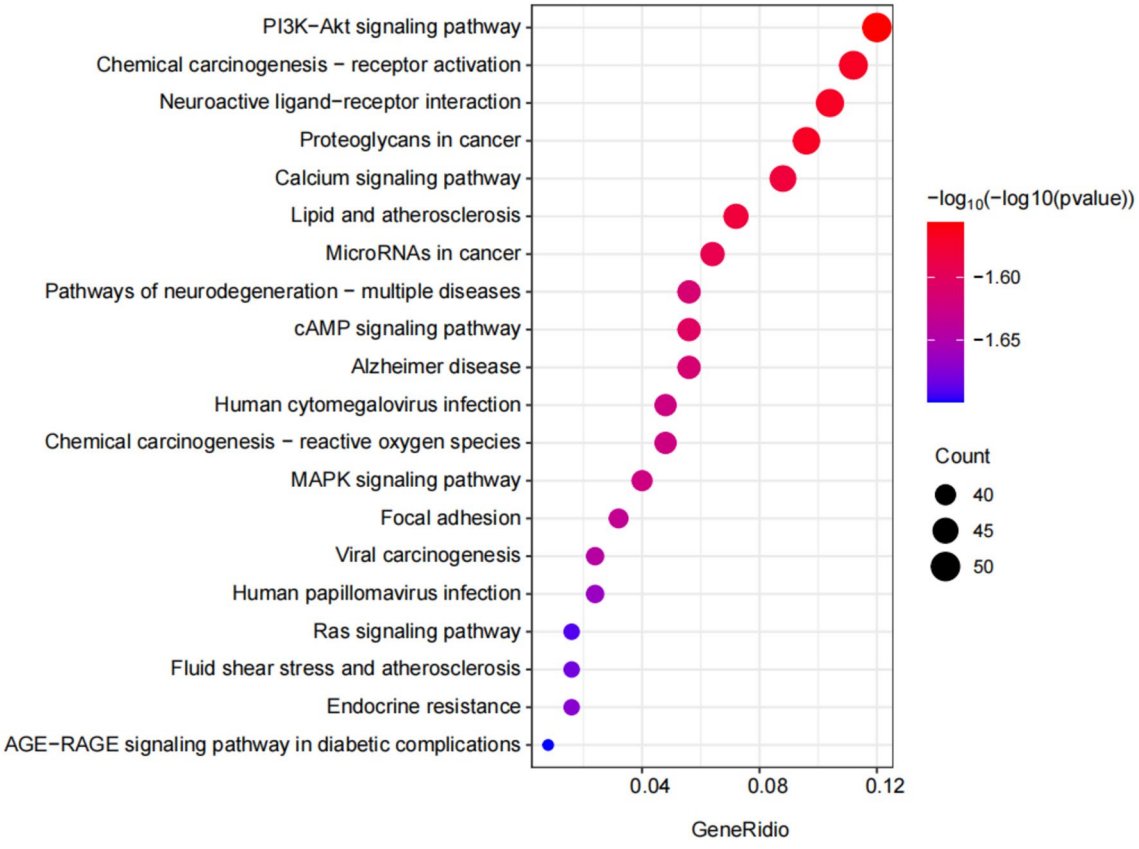

Fig. 4 KEGG pathway enrichment analysis results (the 20 signaling pathways most related to treating PCOS-IR with RD). The larger the circle, the greater the number of genes in the pathway; the redder the color, the more significant the enrichment

number of corpus luteums. These results show that RD can improve the histopathological ovarian changes observed in PCOS-IR rats and that its effect is comparable to that of ME. Additionally, combining RD with Diane-35 is more effective than monotherapy with RD, and provides improvements in ovarian pathology that are similar to those seen with ME(Fig. 10A and F).

RD decreases levels of INS, FBG and HOMA-IR in PCOS-IR rats

Compared with the normal group, model group rats showed significantly elevated serum levels of INS(Fig. 11A), along with significantly higher whole-blood FBG(Fig. 11B) levels and HOMA-IR values (Fig. 11C). Notably, comparison with model group, the decreases in INS, FBG and HOMA-IR levels were comparable between RD-treated PCOS-IR rats and those treated with ME, and between rats treated with RDD-35 and those receiving MED-35(Fig. 11A and C). Combining either RD or ME with Diane-35 was more effective than either RD or ME alone(Fig. 11A and C).

RD improves serum sex hormone levels in PCOS-IR rats

Compared with the normal group, model group rats showed significantly elevated serum levels of LH, T, LH/FSH(Fig. 12A and C), and FSH, E2 levels were significantly reduced (Fig. 12D and E). When compared with the model group, all treatment groups exhibited significantly lower levels of T, LH and LH/FSH (Fig. 12A and C), and FSH, E2 levels were significantly increased (Fig. 12D and E). Notably, the reductions in T, LH, LH/FSH levels and the increases in FSH, E2 levels were uncomparable between RD-treated PCOS-IR rats and those treated with ME, and between rats treated with RDD-35 and those receiving MED-35(Fig. 12A and F). The RDD-35 and MED-35 groups provided greater improvements in T, LH, E2, FSH and LH/FSH levels than RD or ME alone, respectively(Fig. 12A and C).

The effects of RD on the ovarian PI3K/Akt signaling pathway

Western blot analysis revealed that expression levels of the PI3K, p-PI3K, Akt, p-Akt, and GLUT4 proteins in the ovarian tissues of PCOS-IR rats was significantly lower in the Model group than in normal rats (Fig. 13A and F). However, expression of PI3K, p-PI3K, Akt, p-Akt,

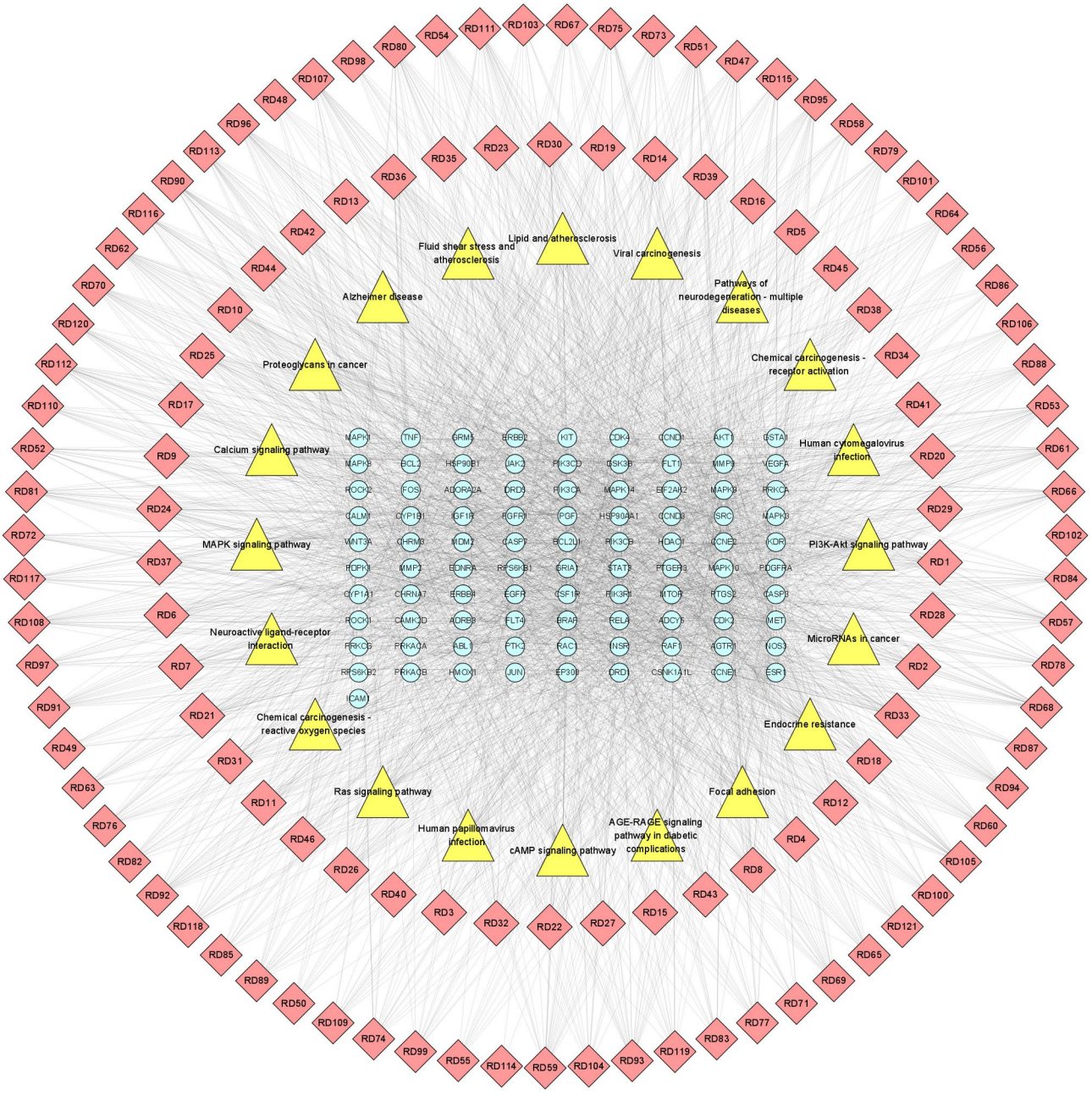

Fig. 5 Compound–target–pathway network. Light blue nodes represent the 91 targets, yellow nodes represent the associated signaling pathways, and pink nodes represent compounds

and GLUT4 was significantly higher in rats in all treatment groups versus the Model group (Fig. 13A and F). The effect of RD on the expression levels of PI3K, p-PI3K, Akt, p-Akt, and GLUT4 proteins in ovarian tissue was comparable to that of ME, and the effect of RDD-35 on these proteins was similar to that of MED-35, with combined therapy showing greater effects than monotherapy with either RD or ME (Fig. 13A and F).Ovarian expression of the FOXO3a and P27 proteins was also significantly higher in Model versus normal rats (Fig. 13G and H), but significantly lower in all treatment groups versus the Model group (Fig. 13G and H). Similar reductions in the expression levels of these proteins were seen in rats treated with RD and ME, and in rats treated with RDD-35 and MED-35(Fig. 13G and H).

RT-qPCR was used to detect the mRNA expression of PI3K, Akt, GLUT4, FOXO3a, and P27 in the ovarian tissues of PCOS-IR rats. When compared with normal rats, Model group rats had significantly lower mRNA expression of PI3K, Akt, and GLUT4 (Fig. 14A and C)

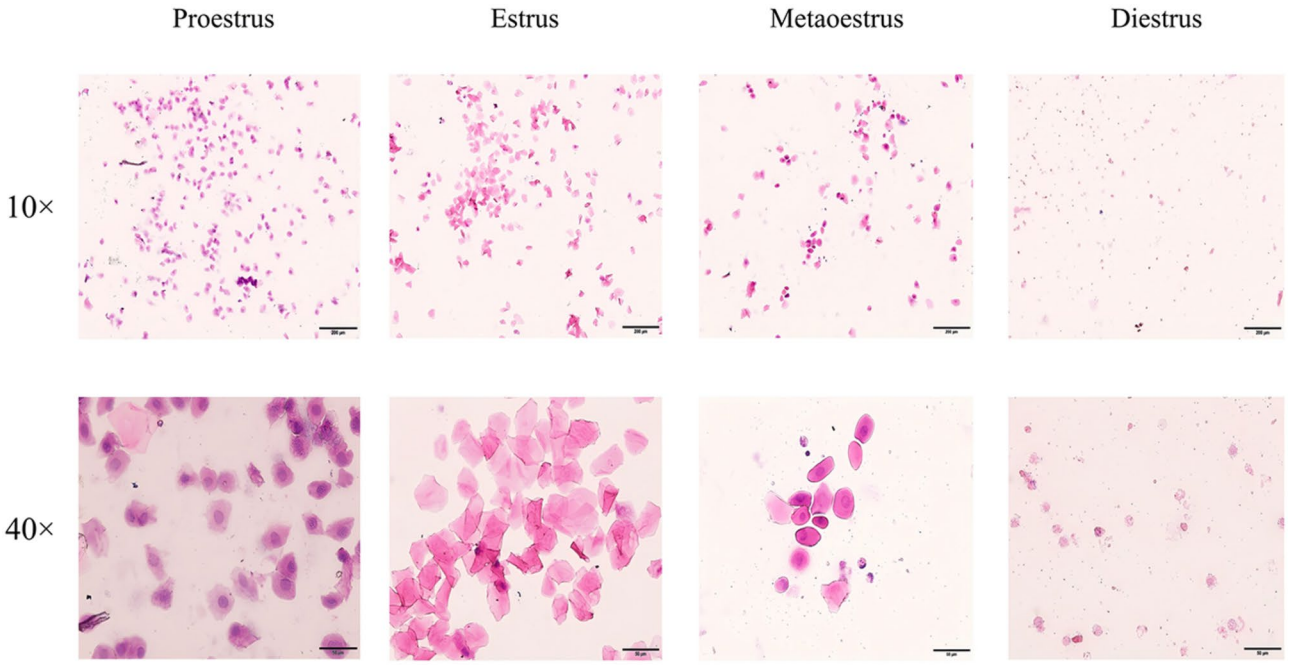

Fig. 6 Vaginal cytologic smears (magnification ×10, ×40) showing the four phases of the estrous cycle in normal rats. Proestrus: large numbers of nucleated epithelial cells; Estrus: large numbers of keratinocytes; Metaoestrus: keratinocytes, nucleated epithelial cells and leukocytes; Diestrus: large numbers of leukocytes

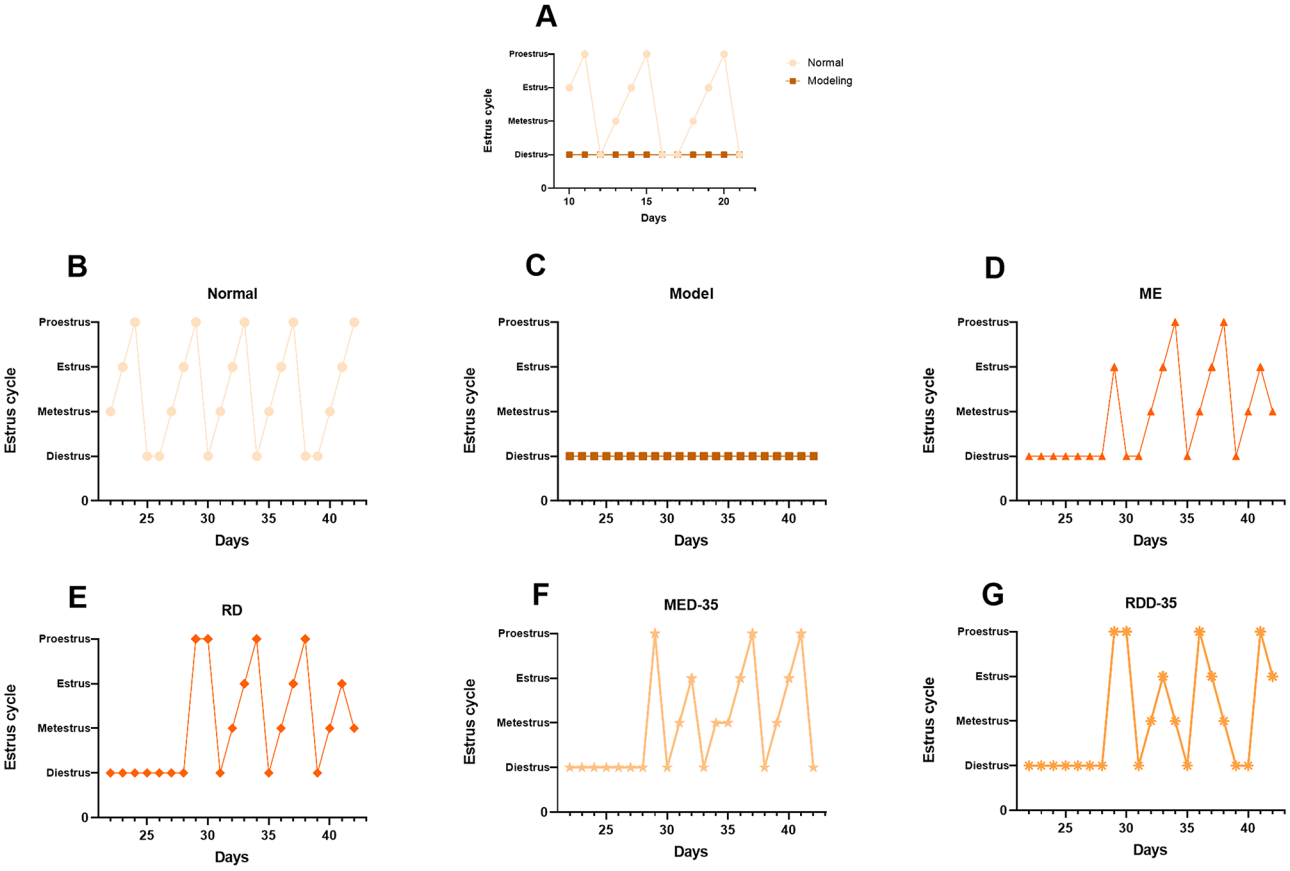

Fig. 7 Estrous cycles in (**A**) normal rats and Model rats during days 10–21; (**B**) normal rats during days 22–42; and (**C**) Model, (**D**) ME, (**E**) RD, (**F**) MED-35, and (**G**) RDD-35 rats during days 22–42

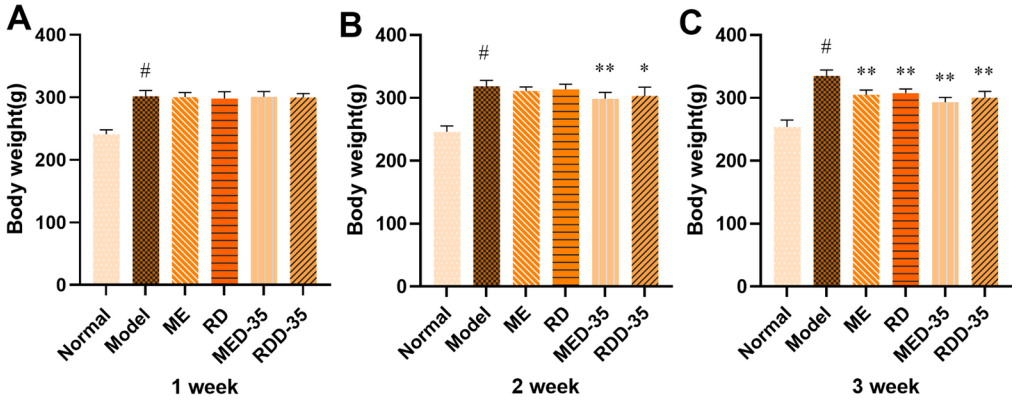

Fig. 8 Effects of RD on body weight in PCOS-IR rats at (**A**) 1 week, (**B**) 2 weeks, and (**C**) 3 weeks after treatment initiation. Values are expressed as mean ± SD ($n = 10$ in each group). $^{\#}P < 0.01$ compared with the normal group. $^{*}P < 0.05$, $^{**}P < 0.01$ compared with the model group

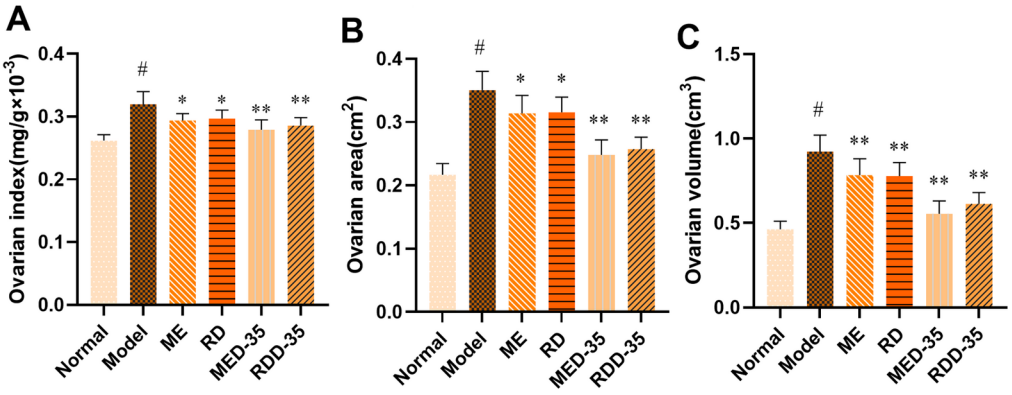

Fig. 9 Effects of RD on (**A**) ovarian index, (**B**) ovarian area, and (**C**) ovarian volume in PCOS-IR rats. Values are expressed as mean ± SD ($n = 10$ in each group). $^{\#}P < 0.01$ compared with the normal group. $^{*}P < 0.05$, $^{**}P < 0.01$ compared with the model group

and significantly higher expression of the FOXO3a and P27 genes (Fig. 14D and F). However, compared with the Model group, the mRNA expression levels of PI3K, Akt, and GLUT4 were significantly increased in all treatment groups (Fig. 14A and C), while the expression of FOXO3a and P27 genes was significantly decreased (Fig. 14D and F).The effect of RD on mRNA expression levels of PI3K, Akt, GLUT4, FOXO3a, and P27 was comparable to that of ME; RDD-35 and MED-35 also had comparable effects on the mRNA expression of these genes, with both combination therapies providing greater effects than RD or ME monotherapy (Fig. 14A and F).

Discussion

RD may improve hyperglycemia, hyperinsulinemia, and insulin resistance in diabetic rats by suppressing chronic inflammation, reducing oxidative stress, and protecting—or promoting the regeneration of—pancreatic β-cells [24]. To date, however, the role of RD in treating PCOS-IR has not yet been studied. This study therefore investigated the effects and the potential mechanisms of action of RD in the treatment of PCOS-IR.

First, we conducted a network pharmacology analysis, which revealed that the treatment of PCOS-IR with RD involves complex interactions among multiple components, targets, and pathways. KEGG pathway enrichment analysis indicated that the PI3K/Akt pathway, a classical pathway for metabolism, is also a key signaling pathway mediating the potential effects of RD in PCOS-IR. In the action of RD on PCOS-IR, key proteins of the PI3K/Akt signaling pathway such as PI3K, Akt, GLUT4, FOXO3a, and P27 may play crucial roles. Under normal conditions, insulin binding to the α-subunit of the insulin receptor activates the β-subunit, which self-phosphorylates on tyrosine residues, thereby activating the insulin receptor substrate (IRS). The activated IRS recruits PI3K, an intracellular phospholipid kinase, and once bound to the IRS, PI3K phosphorylates PIP2 to PIP3 [25]. An increase in PIP3 concentration leads to the recruitment of serine/threonine kinase (Akt) to the cell membrane, resulting in the activation and phosphorylation of Akt. In turn, this promotes the translocation and membrane insertion of glucose transporter 4 (GLUT4), allowing glucose to enter the cell and undergo complete glycolysis [26]. Phosphatidylinositol-3-kinase regulatory subunit 1 (PIK3R1) is

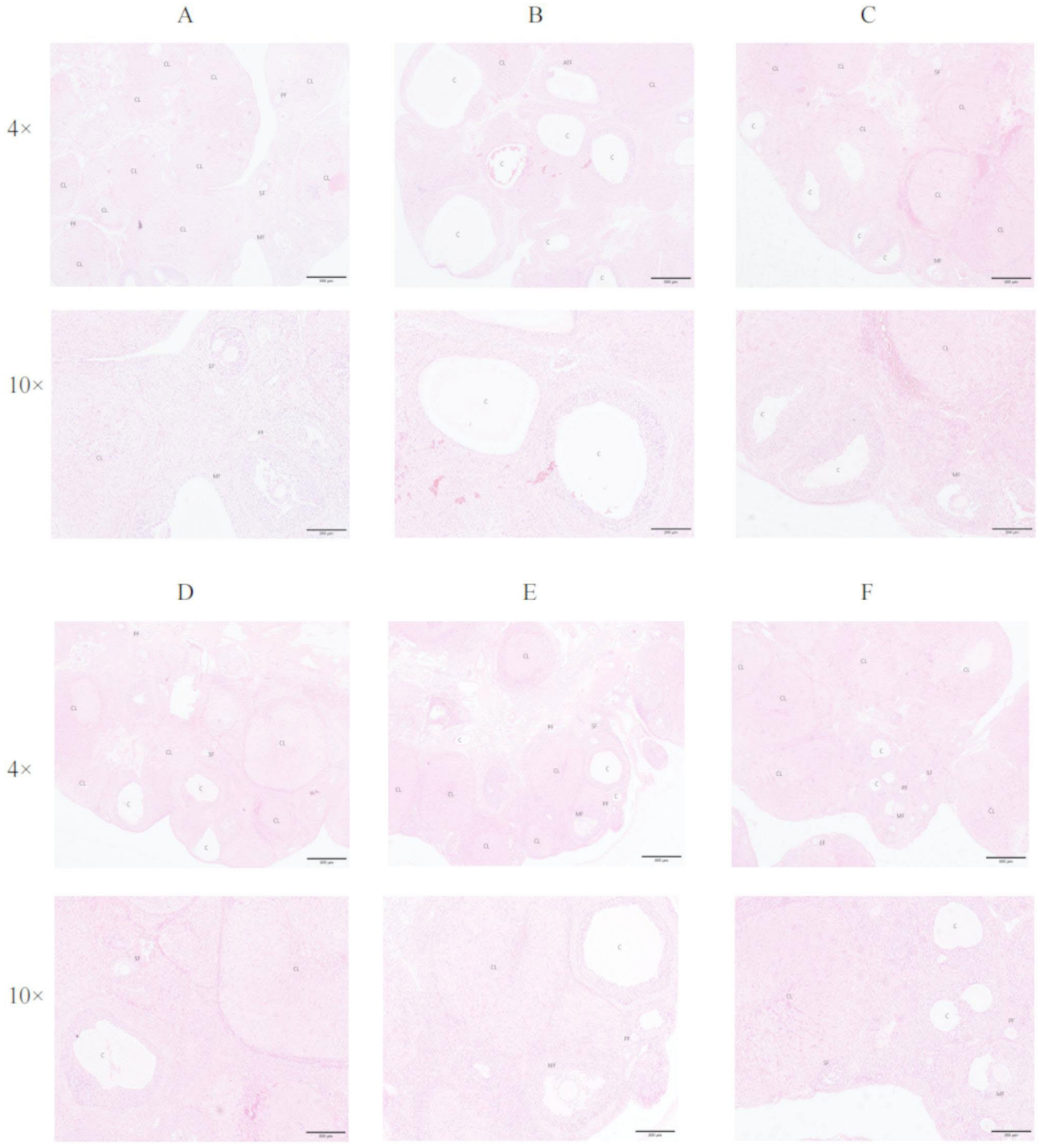

Fig. 10 Effect of RD on ovarian tissue of PCOS-IR rats (HE staining; magnification ×4, ×10). (**A**) Normal group; (**B**) model group; (**C**) ME group; (**D**) RD group; (**E**) MED-35 group; and (**F**) RDD-35 group. CL indicates corpus luteum, C indicates cystic follicle, PF indicates primary follicle, SF indicates secondary follicle and MF indicates mature follicle

an essential component of Class IA PI3K and serves as its regulatory subunit [27], thus playing a positive role in maintaining insulin secretion from β-cells [28]. It has also been identified as an epigenetic marker for the diagnosis of PCOS [29]. Akt is continuously expressed in granulosa cells during their growth, as well as in oocytes [30], and is important for promoting granulosa cell survival, regulating follicular development [31], promoting insulin metabolism [32] and inhibiting the autophagy and apoptosis of ovarian granulosa cells [33]. Akt is in a

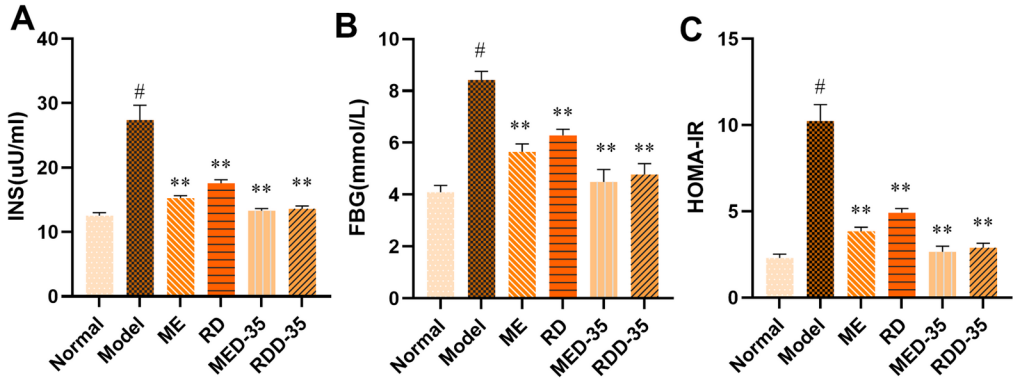

Fig. 11 The Effect of RD on Serum Levels of (**A**) INS and (**B**) FBG, and (**C**) HOMA-IR in PCOS-IR Rats. Values are expressed as mean ± SD ($n = 10$ in each group). #$P < 0.01$ compared with the normal group. *$P < 0.05$, **$P < 0.01$ compared with the model group

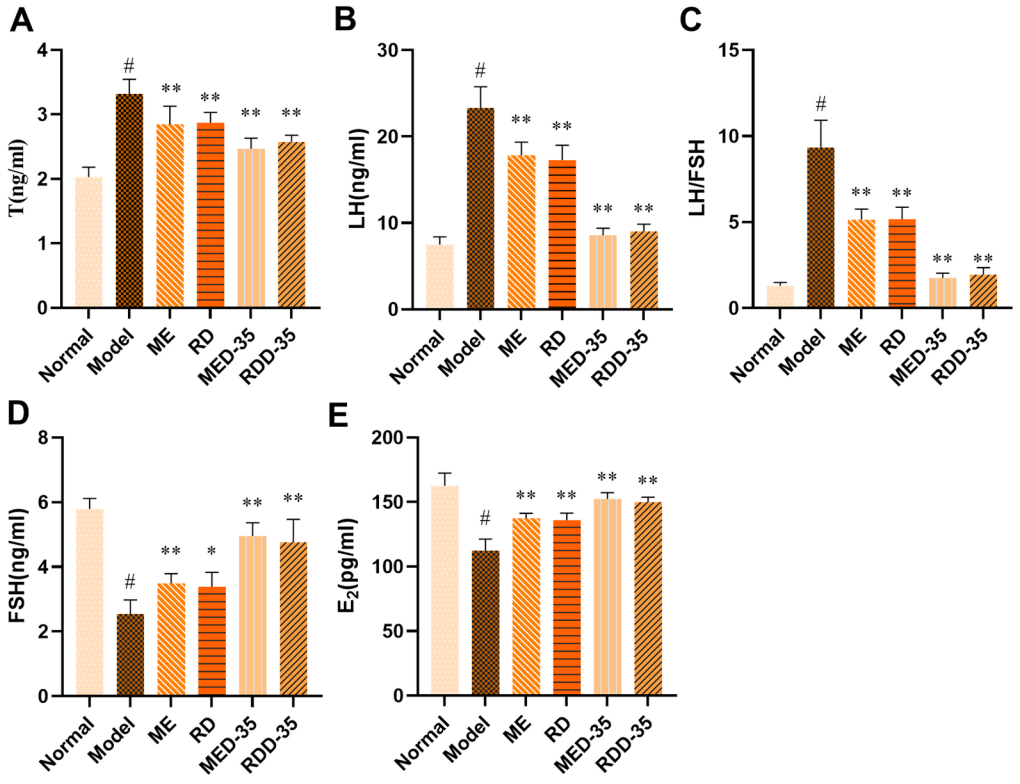

Fig. 12 The Effect of RD on (**A**) T, (**B**) LH, (**C**) LH/FSH, (**D**) FSH, and (**E**) E2 in PCOS-IR Rats. Values are expressed as mean ± SD ($n = 10$ in each group). #$P < 0.01$ compared with the normal group. **$P < 0.01$ compared with the model group

low expression state in PCOS ovarian tissue [34]. Insulin completes glucose uptake through the translocation of GLUT4, a glucose transporter, from intracellular vesicles to the plasma membrane, and this translocation can be stimulated by Akt expression [35]. GLUT4 is expressed in the granulosa cells of primordial and growing follicles in mice and humans [36]; in PCOS patients, the proportion of primordial follicles decreases [37] and GLUT4 is in a low expression state. Forkhead Box O3a (FOXO3a) is a downstream target of the PI3K/Akt pathway known to be widely present in rodent oocytes [38] and involved in the apoptosis of follicles and oocytes [39]. It is in a high expression state in PCOS patients [40]. Akt activation inhibits FOXO3 activation, thereby suppressing oocyte apoptosis [41]. Cyclin-dependent kinase inhibitor 1B (P27), a member of the CDK1 family, is involved in the proliferation and differentiation of various malignant tumor cells in the human body [42]. High expression of P27, as is seen in PCOS patients, inhibits ovarian granulosa cell proliferation [43].

After successfully establishing a PCOS-IR rat model by administering letrozole in combination with a high-fat

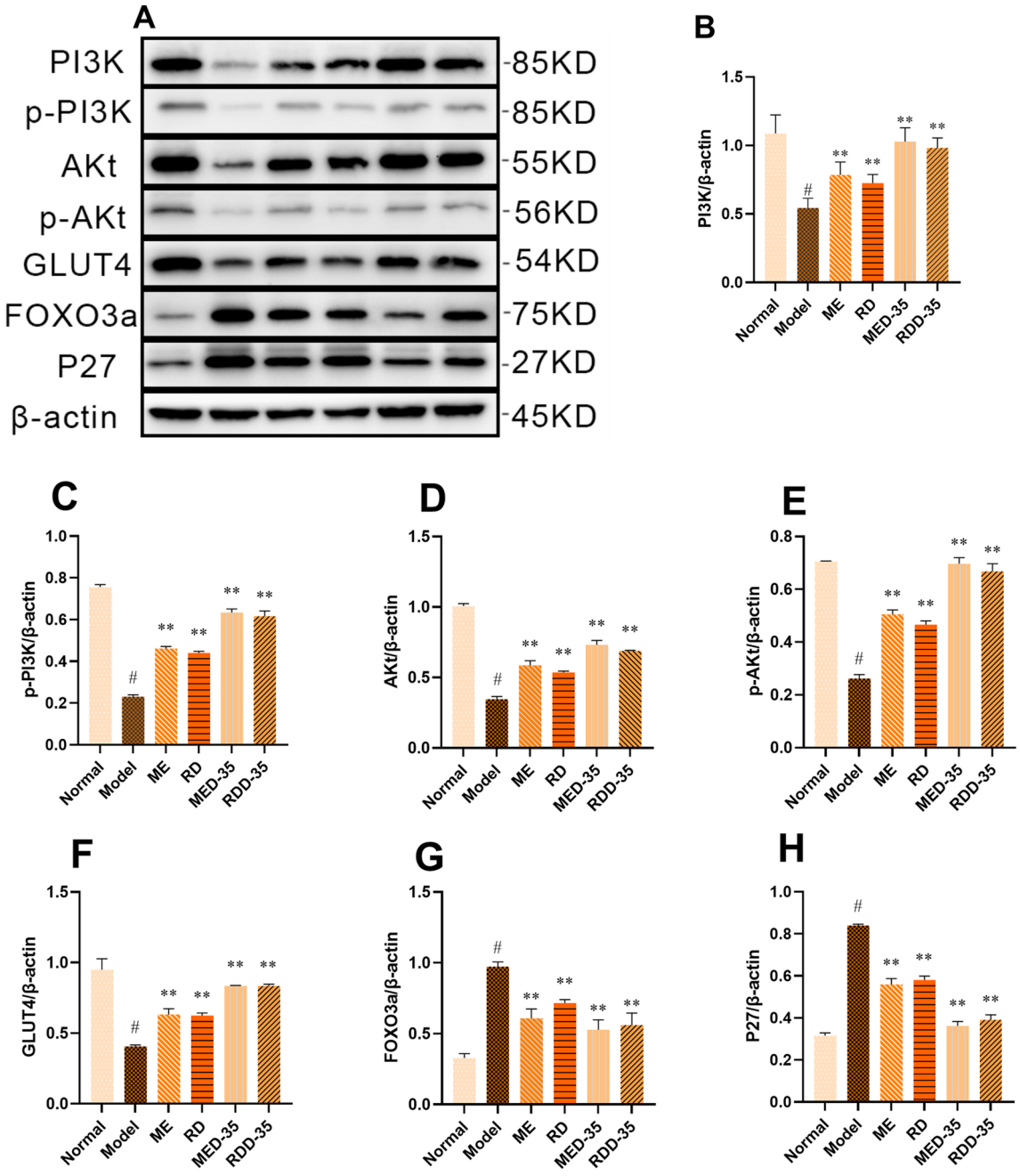

Fig. 13 The Effects of RD on Expression of PI3K/Akt Pathway-Related Proteins in the Ovaries of PCOS-IR Rats. (**A**) Protein expression levels of PI3K, p-PI3K, Akt, p-AKt, GLUT4, FOXO3a, and P27 in ovarian tissue, as detected by Western blot analysis, β-actin was used as control. (**B**) PI3K/β-actin, (**C**) p-PI3K/β-actin, (**D**) Akt/β-actin, (**E**) p-Akt/β-actin, (**F**) GLUT4/β-actin, (**G**) FOXO3a/β-actin, (**H**) P27/β-actin. Results are presented as mean ± SD. $^{\#}P < 0.01$ compared with the normal group. $^{**}P < 0.01$ compared with the model group

diet, we demonstrated that treatment with RD improved ovarian morphology. When compared with ovaries from untreated Model rats, ovaries from RD-treated rats had follicles that displayed the full range of development stages and an increased number of granulosa cell layers. Treatment with RD also improved the pathological morphology of polycystic ovaries, reduced the LH/FSH ratio, increased E2 levels, and reduced T levels. Additionally, we found that RD treatment ameliorated insulin resistance. Experimental validation also revealed that RD significantly increased the expression of PI3K, Akt, and GLUT4 proteins and decreased FOXO3a and P27 expression, thus activating the PI3K/Akt signaling pathway.

Our study also compared the therapeutic effects of RD and ME, alone and in combination with Diane-35, in PCOS-IR rats. Results indicated that there were no

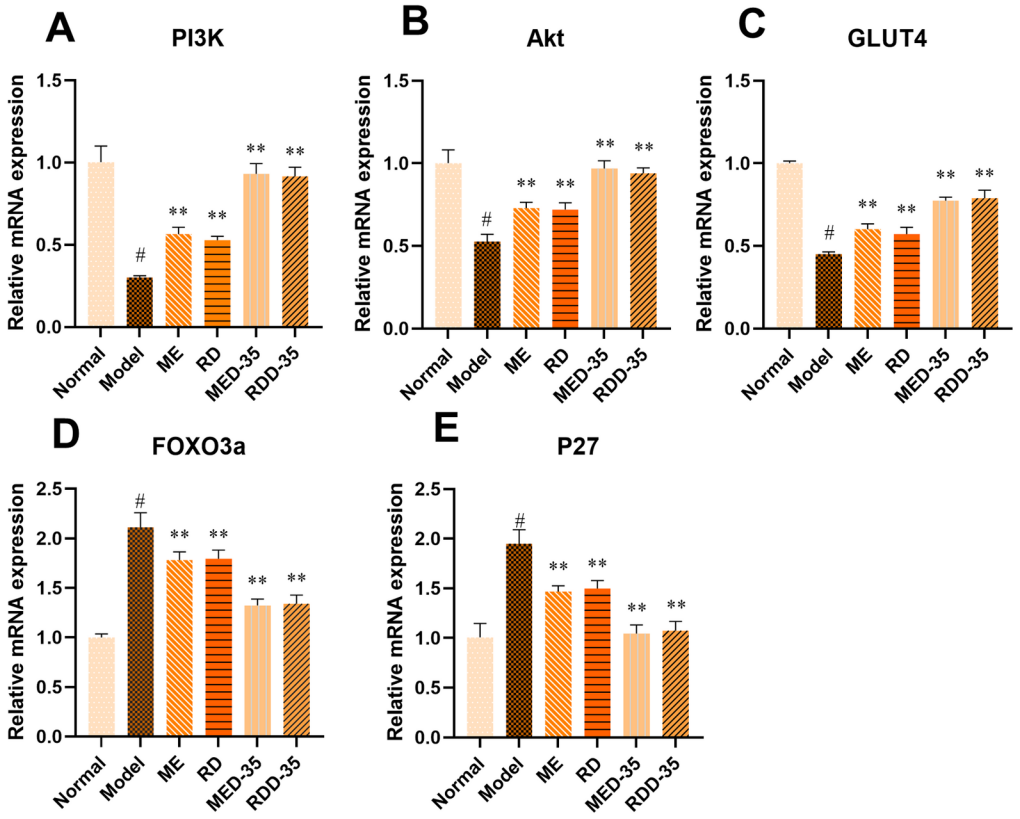

Fig. 14 The effects of RD on PI3K/Akt pathway-related targets in the ovaries of PCOS-IR rats: mRNA expression levels of (**A**) PI3K, (**B**) Akt, (**C**) GLUT4, (**D**) FOXO3a, and (**E**) P27, as detected by RT-qPCR. Values are presented as mean ± SD ($n = 10$ in each group). $^{\#}P < 0.01$ compared with the normal group. $^{**}P < 0.01$ compared with the model group

statistically significant differences in the improvement of insulin resistance, ovarian pathology, and serum sex hormone levels between PCOS-IR rats treated with RD and those treated with ME. Similarly, no significant differences were observed in the same measures between PCOS-IR rats treated with combined RD and Diane-35 (RDD-35) and those receiving combined ME and Diane-35 (MED-35). However, the combined medication approach provided a significantly better improvement in PCOS-IR symptoms than RD or ME monotherapy.

The PI3K/AKt signaling pathway plays an important role in PCOS-IR through glucolipid metabolism [21], and studies have shown that poor lifestyle, obesity and other factors can cause IR by affecting the PI3K/AKt signaling pathway, which not only determines insulin bioactivity, but also affects follicular developmental outcomes. The activated PI3K/Akt pathway regulates follicular apoptosis and promotes follicular maturation [44]. Studies have reported that RD can inhibit tumor cell proliferation and induce apoptosis by modulating the PI3K/AKt signaling pathway in breast and cervical cancer [45, 46]. To investigate whether RD could improve insulin levels in PCOS-IR rats, we examined the expression levels of PI3K, p-PI3K and AKt, p-AKt proteins in the ovarian tissues of PCOS-IR rats, which were similar to the results of a previous study [47], and our findings showed that the expression levels of PI3K, p-PI3K and AKt, p-AKt proteins were significantly reduced compared with those of the normal group significantly decreased, while RD restored PI3K, p-PI3K and AKt, p-AKt protein expression levels to near normal group levels. Meanwhile, changes in serum sex hormone LH, FSH and T levels as well as changes in ovarian morphology also indicated that the PI3K/AKt signaling pathway affects follicular development and maturation, and regulates reproductive function. In conclusion, our study provides new evidence that RD attenuates the pathogenesis of PCOS-IR in a rat model system, which may be related to activation of the PI3K/AKt signaling pathway.

A key limitation of our study is that we focused only on animal studies and the PI3K/Akt signaling pathway to validate the results of our network pharmacology analysis. However, simple animal models may not fully replicate complex human diseases, and PCOS-IR involves multiple targets and pathways. Therefore, future research should include the use of human cell lines and clinical studies to verify the therapeutic effects of RD in patients with PCOS-IR.

Conclusion

In summary, our findings suggest that RD treatment may alleviate symptoms in the PCOS-IR rat model by modulating the PI3K/Akt signaling pathway. This indicates that RD may be a promising therapeutic agent for treating PCOS-IR.

Abbreviations

PCOS	Polycystic ovary syndrome
IR	Insulin resistance
RD	Resina Draconis
PI3K	Phosphatidy linositol 3-kinase
AKt	Protein kinase B
GLUT4	Solute carrier family 2, facilitated glucose transporter member 4
FOXO3a	Forkhead box protein O3
P27	Cyclin-dependent kinase inhibitor 1
GO	Gene Ontology
KEGG	Kyoto Encyclopedia of Genes and Genomes
PPI	Protein-protein interaction
TCM	Traditional Chinese medicine
FSH	Follicle-stimulating hormone
LH	Luteinizing hormone
E2	Estradiol
T	Testosterone
INS	Insulin
FBG	Blood glucose
HOMA-IR	Homeostatic Model Assessment of Insulin Resistance
MED-35	Metformin + Diane-35
RDD-35	Resina Draconis + Diane-35

Supplementary Information

The online version contains supplementary material available at https://doi.org/10.1186/s13048-025-01685-4.

Supplementary Material 1

Supplementary Material 2

Supplementary Material 3

Supplementary Material 4

Supplementary Material 5

Supplementary Material 6

Supplementary Material 7

Supplementary Material 8

Author contributions

J.W. and Y.L. (Yehao Luo): Conceptualization, Methodology, Software, Data Curation, Writing– Original Draft Preparation; Y.L. (Yueting Liu): Methodology, Software, Investigation; X.T., J.H. and Z.H.: Data Curation, Visualization; T.L.: Methodology, Software, Visualization; J.L.:Writing– Review & Editing, Supervision, Project Administration; G.F.:Writing– Review & Editing, Supervision, Project Administration, Funding Acquisition.

Funding

The author(s) declare that financial support was received for the research, authorship, and/or publication of this article. This study was supported by the Guangxi Multidisciplinary Innovation Grant in Traditional Chinese Medicine (No. GZKJ2304); the Guangxi Health Commission Key Laboratory of Applied Fundamental Research of Zhuang Medicine (Guangxi University of Chinese Medicine) (Gui Wei Ke Jiao Fa (2020) No. 17); the Training Program under the "139" Plan for Developing High-level Medical Talent in Guangxi (Gui Wei Ke Jiao Fa (2020) No. 15); and the Guangxi Higher Education Key Laboratory for the Research of Du-related Diseases in Zhuang Medicine (Gui Jiao Ke Yan (2022) No. 10).

Data availability

No datasets were generated or analysed during the current study.

Declarations

Ethics approval and consent to participate

The study was approved by the Ethics Committee of Guangxi University of Chinese Medicine, Nanning, China. Protocol approval number: DW20240603-142.

Consent for publication

Not applicable.

Competing interests

The authors declare no competing interests.

Author details

[1]Guangxi Key Laboratory for Applied Fundamental Research of Zhuang Medicine-Key Laboratory Project under Guangxi Health Commission, Guangxi University of Chinese Medicine, Nanning, Guangxi 530001, China
[2]Guangxi Higher Education Key Laboratory for the Research of Du-related Diseases in Zhuang Medicine, Guangxi University of Chinese Medicine, Nanning, Guangxi 530200, China
[3]Health Science Center, Hubei Minzu University, Enshi 445000, China
[4]School of Second Clinical Medicine, Guangzhou University of Chinese Medicine, Guangzhou 510000, China
[5]Information Technology Center, Guangxi University of Chinese Medicine, Nanning, Guangxi 530001, China

Received: 6 August 2024 / Accepted: 2 May 2025
Published online: 24 May 2025

References

1. Myers SH, Russo M, Dinicola S, Forte G, Unfer V. Questioning PCOS phenotypes for reclassification and tailored therapy. Trends Endocrinol Metab. 2023;34(11):694–703. https://doi.org/10.1016/j.tem.2023.08.005IF:10.9Q1. Epub 2023 Sep 1. PMID: 37661546IF: 10.9 Q1.
2. Li Y, Chen C, Ma Y, Xiao J, Luo G, Li Y, Wu D. Multi-system reproductive metabolic disorder: significance for the pathogenesis and therapy of polycystic ovary syndrome (PCOS). Life Sci. 2019;228:167–75. Epub 2019 Apr 25. PMID: 31029778.
3. Diamanti-Kandarakis E, Dunaif A. Insulin resistance and the polycystic ovary syndrome revisited: an update on mechanisms and implications. Endocr Rev. 2012;33(6):981–1030. doi: 10.1210/er.2011-1034IF: 20.3 Q1. Epub 2012 Oct 12. PMID: 23065822; PMCID: PMC5393155.
4. Wang J, Wu D, Guo H, Li M. Hyperandrogenemia and insulin resistance: the chief culprit of polycystic ovary syndrome. Life Sci. 2019;236:116940. https://doi.org/10.1016/j.lfs.2019.116940. Epub 2019 Oct 8. PMID: 31604107.
5. Poretsky L, Kalin MF. The gonadotropic function of insulin. Endocr Rev. 1987;8(2):132–41. https://doi.org/10.1210/edrv-8-2-132. PMID: 3301317.
6. Dupont J, Scaramuzzi RJ. Insulin signalling and glucose transport in the ovary and ovarian function during the ovarian cycle. Biochem J. 2016;473(11):1483–501. https://doi.org/10.1042/BCJ20160124. PMID: 27234585; PMCID: PMC4888492.
7. Nestler JE. Insulin regulation of human ovarian androgens. Hum Reprod. 1997;12 Suppl 1:53–62. https://doi.org/10.1093/humrep/12.suppl_1.53IF: 6.1 Q1. PMID: 9403321.
8. Armanini D, Boscaro M, Bordin L, Sabbadin C. Controversies in the pathogenesis, diagnosis and treatment of PCOS: focus on insulin resistance, inflammation, and hyperandrogenism. Int J Mol Sci. 2022;23(8):4110. https://doi.org/10.3390/ijms23084110. PMID: 35456928; PMCID: PMC9030414.
9. Fulghesu AM, Romualdi D, Di Florio C, Sanna S, Tagliaferri V, Gambineri A, Tomassoni F, Minerba L, Pasquali R, Lanzone A. Is there a dose-response relationship of metformin treatment in patients with polycystic ovary syndrome? Results from a multicentric study. Hum Reprod. 2012;27(10):3057-66. https://doi.org/10.1093/humrep/des262IF: 6.0 Q1. Epub 2012 Jul 10. PMID: 22786777.
10. Ma F, Qiao L, Yue H, Xie S, Zhou X, Jiang M, Zhang W, Qi J, Wang L, Xu K. Homeostasis model assessment-insulin resistance (HOMA-IR), a key role

for assessing the ovulation function in polycystic ovary syndrome (PCOS) patients with insulin resistance. Endocr J. 2008;55(5):943-5. https://doi.org/10.1507/endocrj.k08e-094IF: 1.3 Q4. Epub 2008 Jun 14. PMID: 18552461.
11. Fan JY, Yi T, Sze-To CM, Zhu L, Peng WL, Zhang YZ, Zhao ZZ, Chen HB. A systematic review of the botanical, phytochemical and Pharmacological profile of Dracaena Cochinchinensis, a plant source of the ethnomedicine Dragon's blood. Molecules. 2014;19(7):10650–69. https://doi.org/10.3390/molecules190710650. PMID: 25054444; PMCID: PMC6270834.
12. Jura-Morawiec J, Tulik M. Dragon's blood secretion and its ecological significance. Chemoecology. 2016;26:101–5. https://doi.org/10.1007/s00049-016-0212-2. Epub 2016 Mar 19. PMID: 27239099; PMCID: PMC4863904.
13. Hu CM, Li JS, Cheah KP, Lin CW, Yu WY, Chang ML, Yeh GC, Chen SH, Cheng HW, Choy CS. Effect of Sanguis draconis (a dragon's blood resin) on streptozotocin- and cytokine-induced β-cell damage, in vitro and in vivo. Diabetes Res Clin Pract. 2011;94(3):417– 25. doi: 10.1016/j.diabres.2011.08.014IF: 5.1 Q2. Epub 2011 Sep 6. PMID: 21899910.
14. Hou Z, Zhang Z, Wu H. Effect of Sanguis draxonis (a Chinese traditional herb) on the formation of insulin resistance in rats. Diabetes Res Clin Pract. 2005;68(1):3–11. doi: 10.1016/j.diabres.2004.08.011. PMID: 15811560.
15. Xu P, Li S, Wu Q, Yang L, Zheng N, Zhu C, Liu P, Li N, Zou L, Loureirin C. from Chinese Dragon's Blood (Dracaena cochinchinensis S.C. Chen), is a novel selective estrogen receptor α modulator with anti-Alzheimer's disease effects. Fitoterapia. 2023;167:105497. https://doi.org/10.1016/j.fitote.2023.105497. Epub 2023 Apr 3. PMID: 37019369.
16. Zhao L, Zhang H, Li N, Chen J, Xu H, Wang Y, Liang Q. Network pharmacology, a promising approach to reveal the pharmacology mechanism of Chinese medicine formula. J Ethnopharmacol. 2023;309:116306. https://doi.org/10.1016/j.jep.2023.116306IF: 5.4 Q1. Epub 2023 Feb 27. PMID: 36858276.
17. Nogales C, Mamdouh ZM, List M, Kiel C, Casas AI, Schmidt HHHW. Network pharmacology: curing causal mechanisms instead of treating symptoms. Trends Pharmacol Sci. 2022;43(2):136–50. Epub 2021 Dec 9. PMID: 34895945.
18. Li S, Zhang B. Traditional Chinese medicine network pharmacology: theory, methodology and application. Chin J Nat Med. 2013;11(2):110– 20. https://doi.org/10.1016/S1875-5364(13)60037-0. PMID: 23787177.
19. Duan ZL, Wang YJ, Lu ZH, Tian L, Xia ZQ, Wang KL, Chen T, Wang R, Feng ZY, Shi GP, Xu XT, Bu F, Ding Y, Jiang F, Zhou JY, Wang Q, Chen YG. Wumei Wan attenuates angiogenesis and inflammation by modulating RAGE signaling pathway in IBD: network Pharmacology analysis and experimental evidence. Phytomedicine. 2023;111:154658. https://doi.org/10.1016/j.phymed.2023.154658. Epub 2023 Jan 12. PMID: 36706698.
20. Zhao H, Chen R, Zheng D, Xiong F, Jia F, Liu J, Zhang L, Zhang N, Zhu S, Liu Y, Zhao L, Liu X. Modified Banxia Xiexin Decoction ameliorates polycystic ovarian syndrome with insulin resistance by regulating intestinal microbiota. Front Cell Infect Microbiol. 2022;12:854796. https://doi.org/10.3389/fcimb.2022.854796. PMID: 35619648; PMCID: PMC9127304.
21. Zhang N, Liu X, Zhuang L, Liu X, Zhao H, Shan Y, Liu Z, Li F, Wang Y, Fang J. Berberine decreases insulin resistance in a PCOS rats by improving GLUT4: dual regulation of the PI3K/AKT and MAPK pathways. Regul Toxicol Pharmacol. 2020;110:104544.
22. Qiu S, Wu C, Lin F, Chen L, Huang Z, Jiang Z. Exercise training improved insulin sensitivity and ovarian morphology in rats with polycystic ovary syndrome. Horm Metab Res. 2009;41(12):880-5. doi: 10.1055/s-0029-1234119IF: 2.2 Q4. Epub 2009 Aug 19. PMID: 19693748IF: 2.2 Q4.
23. Peng MF, Tian S, Song YG, Li CX, Miao MS, Ren Z, Li M. Effects of total flavonoids from Eucommia ulmoides Oliv. Leaves on polycystic ovary syndrome with insulin resistance model rats induced by letrozole combined with a high-fat diet. J Ethnopharmacol. 2021;273:113947. Epub 2021 Feb 19. PMID: 33617969.
24. Chen F, Xiong H, Wang J, Ding X, Shu G, Mei Z. Antidiabetic effect of total flavonoids from Sanguis Draxonis in type 2 diabetic rats. J Ethnopharmacol. 2013;149(3):729–36. Epub 2013 Aug 7. PMID: 23933499.
25. Saltiel AR. Insulin signaling in health and disease. J Clin Invest. 2021;131(1):e142241. doi: 10.1172/JCI142241. PMID: 33393497; PMCID: PMC7773347.
26. Tong C, Wu Y, Zhang L, Yu Y. Insulin resistance, autophagy and apoptosis in patients with polycystic ovary syndrome: association with PI3K signaling pathway. Front Endocrinol (Lausanne). 2022;13:1091147.
27. Du J, Xu Y, Sasada S, Oo AKK, Hassan G, Mahmud H, Khayrani AC, Alam MJ, Kumon K, Uesaki R, Afify SM, Mansour HM, Nair N, Zahra MH, Seno A, Okada N, Chen L, Yan T, Seno M. Signaling inhibitors accelerate the conversion of mouse iPS cells into Cancer stem cells in the tumor microenvironment. Sci Rep. 2020;10(1):9955. https://doi.org/10.1038/s41598-020-66471-2IF:4.6Q2. PMID: 32572057; PMCID: PMC7308356.
28. Tsay A, Wang JC. The role of PIK3R1 in metabolic function and insulin sensitivity. Int J Mol Sci. 2023;24(16):12665. https://doi.org/10.3390/ijms241612665. PMID: 37628845; PMCID: PMC10454413.
29. Zhang F, Ding Y, Zhang B, He M, Wang Z, Lu C, Kang Y. Analysis of methylome, transcriptome, and lipid metabolites to understand the molecular abnormalities in polycystic ovary syndrome. Diabetes Metab Syndr Obes. 2023;16:2745–63. PMID: 37720421; PMCID: PMC10503565.
30. Goto M, Iwase A, Ando H, Kurotsuchi S, Harata T, Kikkawa F. PTEN and Akt expression during growth of human ovarian follicles. J Assist Reprod Genet. 2007;24(11):541–6. https://doi.org/10.1007/s10815-007-9156-3. Epub 2007 Nov 14. PMID: 17999178; PMCID: PMC3455024.
31. Kalous J, Aleshkina D, Anger M. A role of PI3K/Akt signaling in oocyte maturation and early embryo development. Cells. 2023;12(14):1830. https://doi.org/10.3390/cells12141830. PMID: 37508495; PMCID: PMC10378481.
32. Manning BD, Toker A. AKT/PKB signaling: navigating the network. Cell. 2017;169(3):381–405. https://doi.org/10.1016/j.cell.2017.04.001. PMID: 28431241; PMCID: PMC5546324.
33. Tang ZR, Zhang R, Lian ZX, Deng SL, Yu K. Estrogen-Receptor expression and function in female reproductive disease. Cells. 2019;8(10):1123. https://doi.org/10.3390/cells8101123. PMID: 31546660; PMCID: PMC6830311.
34. Qiu Z, Dong J, Xue C, Li X, Liu K, Liu B, Cheng J, Huang F. Liuwei Dihuang Pills alleviate the polycystic ovary syndrome with improved insulin sensitivity through PI3K/Akt signaling pathway. J Ethnopharmacol. 2020;250:111965. https://doi.org/10.1016/j.jep.2019.111965IF: 5.4 Q1. Epub 2019 Jun 8. PMID: 31185267.
35. Kohn AD, Summers SA, Birnbaum MJ, Roth RA. Expression of a constitutively active Akt Ser/Thr kinase in 3T3-L1 adipocytes stimulates glucose uptake and glucose transporter 4 translocation. J Biol Chem. 1996;271(49):31372-8. https://doi.org/10.1074/jbc.271.49.31372. PMID: 8940145.
36. Zhang X, Zhang W, Wang Z, Zheng N, Yuan F, Li B, Li X, Deng L, Lin M, Chen X, Zhang M. Enhanced Glycolysis in granulosa cells promotes the activation of primordial follicles through mTOR signaling. Cell Death Dis. 2022;13(1):87. https://doi.org/10.1038/s41419-022-04541-1IF:.9.0Q1. PMID: 35087042; PMCID: PMC8795455.
37. Webber LJ, Stubbs S, Stark J, Trew GH, Margara R, Hardy K, Franks S. Formation and early development of follicles in the polycystic ovary. Lancet. 2003;362(9389):1017-21. https://doi.org/10.1016/s0140-6736(03)14410-8. PMID: 14522531.
38. Reddy P, Shen L, Ren C, Boman K, Lundin E, Ottander U, Lindgren P, Liu YX, Sun QY, Liu K. Activation of Akt (PKB) and suppression of FKHRL1 in mouse and rat oocytes by stem cell factor during follicular activation and development. Dev Biol. 2005;281(2):160– 70. https://doi.org/10.1016/j.ydbio.2005.02.013. PMID: 15893970.
39. Castrillon DH, Miao L, Kollipara R, Horner JW, DePinho RA. Suppression of ovarian follicle activation in mice by the transcription factor Foxo3a. Science. 2003;301(5630):215–8. https://doi.org/10.1126/science.1086336IF:.56.9Q1. PMID: 12855809.
40. Tan M, Cheng Y, Zhong X, Yang D, Jiang S, Ye Y, Ding M, Guan G, Yang D, Zhao X. LNK promotes granulosa cell apoptosis in PCOS via negatively regulating insulin-stimulated AKT-FOXO3 pathway. Aging. 2021;13(3):4617–33. Epub 2021 Jan 20. PMID: 33495419; PMCID: PMC7906173.
41. Liu H, Luo LL, Qian YS, Fu YC, Sui XX, Geng YJ, Huang DN, Gao ST, Zhang RL. FOXO3a is involved in the apoptosis of naked oocytes and oocytes of primordial follicles from neonatal rat ovaries. Biochem Biophys Res Commun. 2009;381(4):722-7. https://doi.org/10.1016/j.bbrc.2009.02.138. Epub 2009 Mar 1. PMID: 19258007.
42. Hnit SS, Xie C, Yao M, Holst J, Bensoussan A, De Souza P, Li Z, Dong Q. p27(Kip1) signaling: Transcriptional and post-translational regulation. Int J Biochem Cell Biol. 2015;68:9–14. https://doi.org/10.1016/j.biocel.2015.08.005IF: 4.0 Q2. Epub 2015 Aug 14. PMID: 26279144.
43. Zhao J, Xu J, Wang W, Zhao H, Liu H, Liu X, Liu J, Sun Y, Dunaif A, Du Y, Chen ZJ. Long non-coding RNA LINC-01572:28 inhibits granulosa cell growth via a decrease in p27 (Kip1) degradation in patients with polycystic ovary syndrome. EBioMedicine. 2018;36:526–538. https://doi.org/10.1016/j.ebiom.2018.09.043. Epub 2018 Oct 5. Erratum in: EBioMedicine. 2018;37:563. PMID: 30293818; PMCID: PMC6197751.
44. Li M, Gao S, Kang M, Zhang X, Lan P, Wu X, Yan X, Dang H, Zheng J. Quercitrin alleviates lipid metabolism disorder in polycystic ovary syndrome-insulin resistance by upregulating PM20D1 in the PI3K/Akt pathway. Phytomedicine. 2023;117:154908.

45. Hong Y, Sun X, Lu L. Loureirin B inhibits cervical Cancer development by blocking PI3K/AKT signaling pathway: network Pharmacology analysis and experimental validation. Appl Biochem Biotechnol. 2024;196:8587–604.
46. Lv Y, Mou Y, Su J, Liu S, Ding X, Yuan Y, Li G, Li G. The inhibitory effect and mechanism of Resina draconis on the proliferation of MCF-7 breast cancer cells: a network pharmacology-based analysis. Sci Rep. 2023;13:3816.
47. Li T, Mo H, Chen W, Li L, Xiao Y, Zhang J, Li X, Lu Y. Role of the PI3K-Akt signaling pathway in the pathogenesis of polycystic ovary syndrome. Reprod Sci. 2017;24:646–55.

Publisher's note